J. Fluid Mech. (2012), *vol.* 701, *pp.* 473–481. © Cambridge University Press 2012
doi:10.1017/jfm.2012.188

On the flow field induced by a hovering rotor or a static jet

Philippe R. Spalart†

Boeing Commercial Airplanes, PO Box 3707, Seattle, WA 98124, USA

(Received 14 October 2011; revised 27 January 2012; accepted 16 April 2012;
first published online 10 May 2012)

The flow in the far field of an isolated static momentum source is considered, taking into account the entrainment of fluid by the turbulent jet which develops far downstream irrespective of the type of device. The result is a simple analytical model for the irrotational region, which depends only on the thrust applied. This equation is implied by Stewart (*J. Fluid Mech.*, vol. 1, 1956, pp. 593–606) for a jet. For a rotor, the model is radically different from the classical one derived from an actuator disk without turbulence or mixing in the wake, which led to a sink flow in the far field. The velocities decay like $1/r$ rather than $1/r^2$, where r is the radius, and are everywhere directed in the direction opposite to the thrust, rather than pointing towards the origin. The momentum source drives a co-flow which converges towards the turbulent region, thus supplying the entrained fluid. This flow pattern supports the assumption that the fluid surrounding the turbulent region is irrotational, better than the sink-flow model would. The model depends only on one empirical constant, a measure of the entrainment in a fully developed jet, for which a range of values is determined from the experimental literature. If the rotor is climbing, the sink flow is recovered; however, the limit of that equation as the climb velocity tends to zero, leading to hover, is singular. For both jets and rotors, this model used in a boundary condition should eliminate extraneous parameters and reduce the computational cost of numerical simulations, and may guide the design of chambers used for experiments, following Ricou & Spalding (*J. Fluid Mech.*, vol. 11, 1960, pp. 21–32).

Key words: general fluid mechanics, mathematical foundations, wakes/jets

1. Introduction

The discussion will use the orientation and vocabulary of a helicopter rotor, and the application to jets will be addressed in due course. In past work (Spalart 2003) we believe we improved on the textbook description of the flow around the rotor, purely with an actuator–disk model and a steady, inviscid streamtube, leading to a radial sink flow at large distances and exact statements of momentum conservation over large control volumes. The volume flow Q_0 of the sink is known from the classical literature from the density ρ, rotor radius R, and thrust T: $Q_0 = R\sqrt{\pi T/(2\rho)}$. Simulations also agree qualitatively with our prediction that the vortex sheet first lifts at the rim of the rotor, and then dives through the rotor disk (Buning & Chaderjian 2011); the highlight

† Email address for correspondence: philippe.r.spalart@boeing.com

https://doi.org/10.1017/jfm.2012.188 Published online by Cambridge University Press

of our 2003 work was that, especially in hover, the velocity across the disk is far from uniform, contrary to the textbook descriptions. This concerns the near field.

In the far field, a definite weakness of this inviscid actuator–disk model is its conflict with the fact that the wake is surely turbulent, ultimately evolving into a self-similar jet, inside which the volume flow increases linearly with the streamwise distance x, if classical turbulence theory is correct. Therefore the volume flow Q_0 through the rotor disk loses its relevance once the radius δ of the wake far exceeds R and the local volume flow Q far exceeds Q_0. In the turbulent far wake of the rotor, which is a jet flow, the dominant parameter is $\sqrt{T/\rho}$, with dimension length^2/time, and the decay of the peak velocity follows $\sqrt{T/\rho}/x$, indicating that the $1/x^2$ behaviour of the sink flow is superseded. Here, we are using the traditional physical model and dimensional analysis of the fully developed turbulent jet, and adding that at large enough distances the local Mach number is low, thus justifying an incompressible treatment. Note also that if a jet is considered instead of a rotor, the mass flow supplied by the jet also loses relevance at large distances. In fact, a jet engine has a negligible added mass flow (that of the fuel) and is thus closer to a rotor flow than to a laboratory jet flow with a gas supply.

The conceptual model and scaling laws of the turbulent jet as a thin shear flow are well known, but the global flow field in directions other than downstream appears not to be prominent in recent jet literature, and to be simply absent from helicopter literature. A good model for it will be valuable for numerical simulations, primarily to reduce the required domain size and to guide the type of boundary condition applied in each region, with typically a choice between ‘inflow’ and ‘outflow’. The actuator–disk sink model leads to inflow conditions in all directions except directly downstream. It is available in some rotor codes (Strawn & Ahmad 2000), but is certainly not universally used (Buning & Chaderjian 2011). In addition, simulation results do not support the prediction that the flow direction just outside the wake is towards the rotor and therefore upwards (N. Chaderjian, personal communication, 2011). Boundary conditions as well as initial conditions closer to the true behaviour of the flow may also shorten the initial transients, and improve the prediction of the induced power, which is sensitive to the downwash.

These considerations motivated a new effort with the simple task of finding the analytical model for the far-field flow, driven by the quantity $\sqrt{T/\rho}$, and compatible with the thin-shear-flow model of the turbulent jet. Dimensional analysis immediately created an expectation for $1/r$ decay of the velocities, therefore extremely different from that of a sink flow in three dimensions and incompatible with actuator–disk discussions in textbooks and by Spalart (2003). This expectation was confirmed by the differential equations and their solutions, and is at the core of the article.

The model is axisymmetric, not because the geometry is, but by the assumption that in the far field the flow loses memory of the geometric details, so that only the thrust vector is material. For instance, rectangular jets are widely assumed to relax to an axisymmetric state far enough from the nozzle. To be precise, T is the total force of the flow or lift of the aircraft, which may include both rotor thrust and download on the airframe. Thus, a set of jets or a helicopter with tandem rotors are also targets of the present model, although this loss of memory will take a longer distance than for a nominally axisymmetric momentum source. On the other hand, only static rotors and jets are considered, until a rotor in a climb is revisited in § 3.

https://doi.org/10.1017/jfm.2012.188 Published online by Cambridge University Press

2. Far-field model

2.1. *Mathematical development*

To analyse the present axisymmetric flows, we use spherical coordinates (r, θ, ϕ) and cylindrical coordinates (x, y, ϕ), with the ϕ-dependence omitted. Let the thrust point in the $\theta = 0$, positive x, direction; for the rotor, this is upwards. A Stokes stream function $\Psi(r, \theta)$ is introduced such that

$$u_r = \frac{1}{r^2 \sin\theta} \frac{\partial \Psi}{\partial \theta}, \quad u_\theta = -\frac{1}{r \sin\theta} \frac{\partial \Psi}{\partial r}. \tag{2.1}$$

Since the rotor or jet is the only source of vorticity, we naturally expect irrotational flow outside the rotor region, that is, except in the wake near $\theta = \pi$; this assumption will be revisited. The zero-vorticity condition gives the equation $\omega_\phi = [r^2 \Psi_{rr} + \sin\theta \partial_\theta (\Psi_\theta / \sin\theta)]/[r^3 \sin\theta] = 0$. If the velocity scales like $1/r$ and the solution is separable, the stream function scales like r, so that $\Psi_{rr} = 0$, and the θ dependence satisfies $\partial_\theta (\Psi_\theta / \sin\theta) = 0$. This linear second-order equation has two solutions: a constant, and $\cos\theta$, giving Ψ proportional to r and to x respectively. Due to the presence of $\sin\theta$ in the denominator of (2.1), the only combination that produces a regular velocity field at $\theta = 0$, above the rotor, is $\Psi = r(1 - \cos\theta) = r - x$. The sink flow has $\Psi \propto (\cos\theta - 1)$, making it the x-derivative of the $(r - x)$ solution. Then, by dimensional analysis, $\Psi = -A\sqrt{T/\rho} r(1 - \cos\theta)$, and so from (2.1)

$$u_r = -\frac{A}{r}\sqrt{\frac{T}{\rho}}, \quad u_\theta = \frac{A}{r}\sqrt{\frac{T}{\rho}} \tan\left(\frac{\theta}{2}\right), \tag{2.2}$$

where A is a non-dimensional constant. This is our key result. The $1/r$ dependence is confirmed. Stewart (1956), in his discussion of static jets, went through the same steps and gave the streamlines for this same flow, although not explicitly the velocity field. He did not discuss the value of A. This is the flow induced by a semi-infinite line of sinks of density $\mathrm{d}Q/\mathrm{d}x = 4\pi A\sqrt{T/\rho}$ on the $\theta = \pi$ semi-axis (Crow & Champagne 1970); the velocity is singular there. Thus, A is a universal constant which is a measure of the entrainment rate of a low-speed fully developed turbulent jet.

Jet experiments suggest for A values between 0.022 and 0.032 (Ricou & Spalding 1960; Schlichting 1979; Falcone & Cataldo 2003) and we use the median 0.027 from here on. Some studies suggest the lower values found for A are the consequence of insufficient development of the jet; conversely, it seems that the higher value (0.032) has not been repeated, and could result from neglecting precisely the surrounding flow field we are studying here (Crow & Champagne 1970). Thus, the plausible range is not as wide as [0.022,0.032]. This concerns the exact value. Each turbulence model has its own value of A, which can deviate appreciably from the exact one.

The laminar jet solution is given by Schlichting (1979). The power laws for jet width and velocity are the same as for turbulent flow, so that the volume flow also grows linearly with x, equalling $Q = 8\pi\nu x$. As a result, the effective A of a laminar jet is $2/Re$, where $Re \equiv \sqrt{T/\rho}/\nu$ is a Reynolds number of the jet. Even a laminar jet has a $1/r$ far-field behaviour, inside and outside the viscous region.

Note that for a classical actuator disk the key quantity $\sqrt{T/\rho}$ is equal to $\sqrt{2\pi} R v_h$, where R is the disk radius, and v_h is the standard velocity in hover, a useful reference as it sets the induced power, $P_i = T v_h$. The model applies where $r \gg R$, and therefore $|u| \ll v_h$ from (2.2). This is consistent.

https://doi.org/10.1017/jfm.2012.188 Published online by Cambridge University Press

To include the vortical region near $\theta = \pi$, the Stokes stream function Ψ is modified by a function $f(\theta)$, which will be adjusted to fit the universal profile of a fully developed jet: $\Psi = -A\sqrt{T/\rho}r(1 - \cos\theta)f(\theta)$, where $f = 1$ outside the wake and $f = O((\pi - \theta)^2)$ for $\theta \to \pi$. This amounts to a composite asymptotic expansion in the θ direction, but without any attempt at fully solving the inner problem near $\theta = \pi$, for the simple reason that it contains turbulence and has no analytical solution. The function f is empirical and will become better known from experiments and direct numerical simulations, and the key measure of it that is needed in practice is simply A. With $f(\pi) = 0$, we have $\Psi(r, 0) = \Psi(r, \pi) = 0$, so that mass is conserved, and the velocity is now smooth on the entire x axis (because of the quadratic dependence of Ψ near both $\theta = 0$ and $\theta = \pi$) and therefore in all of space except at the origin. Then,

$$u_r = -\frac{A}{r}\sqrt{\frac{T}{\rho}}\left[f(\theta) + \tan\left(\frac{\theta}{2}\right)\frac{\mathrm{d}f}{\mathrm{d}\theta}\right], \quad u_\theta = \frac{A}{r}\sqrt{\frac{T}{\rho}}\tan\left(\frac{\theta}{2}\right)f(\theta). \tag{2.3}$$

Compare with (2.2).

The velocity field has been covered. In the irrotational region, the pressure is given by Bernoulli's equation applied to (2.2), $p = p_\infty - \rho\|u\|^2/2$, so that

$$p = p_\infty - \frac{T}{r^2}\frac{A^2}{2\cos^2(\theta/2)}. \tag{2.4}$$

In compressible simulations, (2.4) is a good approximation in the far field, and the density and temperature can be obtained from the isentropic relations. To obtain a model usable over the entire domain, (2.4) will require a plausible regularization near $\theta = \pi$, as it is highly singular because of the line sink. One possibility would be to multiply the second term in the right-hand side by f. Unfortunately, this uncertainty over the pressure in the turbulent region puts simple expressions for a full three-dimensional control-volume analysis of momentum out of reach, unlike in the situation with the sink flow (Spalart 2003). The pressure in the jet depends on the Reynolds stresses, which also enter the momentum balance in their own right, so that detailed empirical models would be needed beyond that for the velocity profile.

2.2. *Illustration and comparison with data*

Figure 1 shows the streamlines of this flow with the Gaussian function $f(\theta) = 1 - \exp(-[(\pi - \theta)/\sigma]^2)$, with $\sigma = 0.135$ which provides a reasonable fit to the width of turbulent jets. The link between A and σ will be explained shortly. In this figure, the region near the origin is not shown, because this is where the approximation is not valid. The radius of this deviation region will be at least several rotor diameters.

Observe the direction of the flow outside the wake, everywhere downwards and towards the axis. The velocity components in cylindrical coordinates do not switch sign. The axial component of (2.2) is $u_x = -A\sqrt{T/\rho}/r$; it is constant at a given distance r, and always in the direction opposite to the thrust, in strong contrast with the sink-flow model. All the fluid is coming from above the rotor. Similarly, the velocity component u_y away from the cylindrical axis is $u_y = -A\sqrt{T/\rho}\tan(\theta/2)/r$ and is everywhere negative. Close to the jet ($\theta \to \pi$) it equals approximately $-2A\sqrt{T/\rho}/y$, and is thus inversely proportional to y (a two-dimensional sink) and independent of x, as verified experimentally by Falcone & Cataldo (2003). Fluid is also, in fact predominantly, coming from the lateral direction (Stewart 1956). This is very

https://doi.org/10.1017/jfm.2012.188 Published online by Cambridge University Press

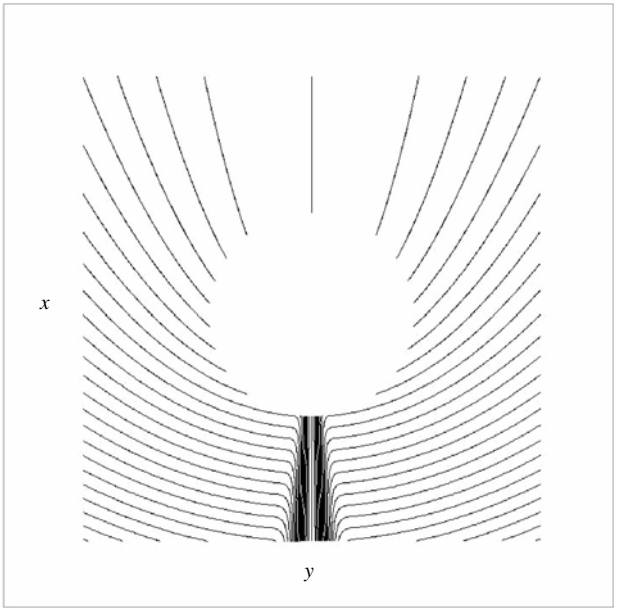


FIGURE 1. Streamlines of the far-field model. They all point downward.

favourable for the consistency of the irrotational assumption: fluid does not 'creep back' up towards the origin along the vortical turbulent region as it would with the sink-flow model. If it did, that would raise concerns that it might acquire vorticity and turbulence in the process.

We have not been able to find rotor experiments or simulations which specifically support the $1/r$ dependence, or a $1/r^2$ dependence for that matter. However, rotor simulations by Dziubinski and Stalewski using an actuator disk and a turbulent wake are in excellent quantitative agreement over the streamline shapes (Dziubinski & Stalewski 2007).

Jet simulations are more helpful, as seen in figure 2, derived from a line of large-eddy simulations (Shur, Spalart & Strelets 2011). This simulation had a jet Mach number of 0.9 and a weak co-flow of 3×10^{-3} of the jet velocity. The far-field conditions did not use the new model *per se*, but did use an extrapolation of the u_y component according to a $1/y$ law along the lateral boundary. The u_x velocity was uniformly set to the co-flow value both at the upper and lateral boundaries, and its value matches the new model at a distance $r \approx 8D$. Since the boundaries are at about $r = 20$–$25D$, this co-flow is much stronger than the natural one. Therefore, the behaviour at intermediate distances constitutes a largely independent test of that model. The streamline shapes in the left graph are very convincing when compared with figure 1. Near $x/D = 30$, at the edge of the jet, the radial velocity $-u_y$ is $\sim 7 \times 10^{-3}$ so that the co-flow of 3×10^{-3} deflects the streamlines downwards; for smaller values of x/D this effect is seen to vanish. In addition, the $1/r$ behaviour of the velocity component $-u_y$ directed towards the axis is very clear over a wide range in the right graph. The figure suggests for the fully developed region a value of ~ 0.26 for $\mathrm{d}Q/\mathrm{d}x$, in the units used; in the same units, $\sqrt{T/\rho_\infty}$ equals 0.863. This corresponds to $A \approx 0.023$, a value which is within the experimental range we have determined. Therefore, the jet simulations are highly supportive of the model.

https://doi.org/10.1017/jfm.2012.188 Published online by Cambridge University Press

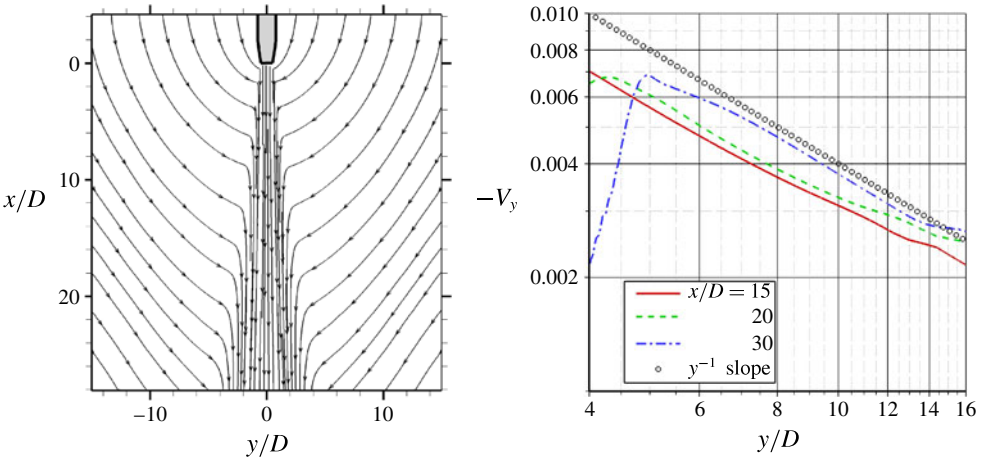


FIGURE 2. (Colour online available at journals.cambridge.org/flm) Results of a jet large-eddy simulation, courtesy of Dr M. Shur. (*a*) Streamlines; (*b*) radial velocity in cylindrical coordinates.

2.3. *Flow inside the wake*

The velocity of the jet itself is defined as the deviation from the irrotational field at the same location, therefore the difference between the x-components of (2.3) and of (2.2):

$$u_{jet} = -\frac{A}{r}\sqrt{\frac{T}{\rho}}\left[f(\theta) - 1 + \cos\theta \tan\left(\frac{\theta}{2}\right)\frac{\mathrm{d}f}{\mathrm{d}\theta}\right]. \tag{2.5}$$

It is close to Gaussian for θ near π if $(1-f)$ is Gaussian.

Crow & Champagne (1970) explain this concept of a deviation or 'excess' velocity introduced in (2.5), derived from the composite expansion. Curiously, they use the excess over an approximation to (2.2) instead of (2.2) itself, namely $u_x = A\sqrt{T/\rho}/y$, an approximation which is valid only when $y \gg x$ (i.e. $\theta \to \pi/2$). This approximation is not valid at all just outside the jet. This might in fact be a typographical confusion in the article between spherical and cylindrical coordinates, both often using r.

The thrust of the jet profile given by (2.5), in the thin-layer approximation, is

$$T_{tl} = \rho \int\int u_{jet}^2 \,\mathrm{d}y\,\mathrm{d}z = 2\pi A^2 T \int_0^\pi \left[f(\theta) - 1 + \cos\theta \tan\left(\frac{\theta}{2}\right)\frac{\mathrm{d}f}{\mathrm{d}\theta}\right]^2 \sin\theta\,\mathrm{d}\theta. \tag{2.6}$$

This equation dictates the value of A for any choice of f, as the value of T_{tl} given by (2.6) must equal T, which is found just before the $\int$ sign. Equation (2.6) is the matching condition between f and A, and it was applied to pick the width σ of the Gaussian in figure 1 consistent with $A = 0.027$, namely $\sigma = \sqrt{8\pi}A$. The Gaussian then gives a peak velocity near $6\sqrt{T/\rho}/x$, which is somewhat too low because its shape is not very accurate. However, the crucial empirical constant is A, which sets the magnitude of the velocity in all directions outside the jet itself.

Based on experiments, the peak velocity of the jet at distance x is ~8–10 times $\sqrt{T/\rho}/x$ while the ambient x velocity it is surrounded by is near $0.027\sqrt{T/\rho}/x$. The ratio between the two is very large, so that the present effect is hardly measurable in experiments or detectable in simulations via the x velocity. The y velocity at the edge of the Gaussian with $\pi - \theta \approx 0.15$ is larger, roughly $0.3\sqrt{T/\rho}/x$, which is also far

https://doi.org/10.1017/jfm.2012.188 Published online by Cambridge University Press

smaller than the jet velocity, but at 3 % is measurable (Falcone & Cataldo 2003). The predictions of the model are difficult (but not impossible) to confirm quantitatively in experiments, ultimately because a jet is a thin shear flow, which gave the key constant A a small value. Thus (2.6) is more effective, but it is iterative, since a value of A is needed to define the excess velocity.

3. Significance

The model presented here, while the $1/r$ dependence of the velocity magnitude came as a surprise in the context of rotors, is convincing mathematically and consistent with classical articles on jets. Perspective may be gained in the helicopter context by comparing the hover case with neighbouring cases in climb (descent is less convincing, because the wake will turn around instead of smoothly extending to infinity as it does in climb). Let the climb velocity be U_0, and let u_{max} be the peak downward excess velocity on the centreline under the rotor, which decays like $|x|^{-2/3}$ by dimensional analysis since we now have an axisymmetric wake instead of a jet. In the far wake, where $u_{max} \ll U_0$, a linearized momentum balance shows that the thrust is simply U_0 times the mass flow ρQ of the wake, which here is constant instead of growing linearly as it does in the hover case. Finally, the irrotational far-field flow is a sink again:

$$u_r = -\frac{T}{\rho U_0}\frac{1}{4\pi r^2}. \tag{3.1}$$

Remarkably, this sink field does not depend on the turbulence: there is no empirical constant equivalent to A, and the flow could be laminar. Turbulence has an effect on the flow inside the wake, but not outside it. Actually, in as much as the Reynolds number of the flow decays like $x^{-1/3}$ for large distances, the flow should be expected ultimately to revert to laminar. Thus, it turns out that turbulent mixing makes a major difference in the far field only for the hover case.

The crucial point is that, at fixed T and r, when approaching hover so that $U_0 \to 0$, (3.1) diverges. In other words, the limit of the behaviour in climb when the climb rate vanishes is singular, which makes it less surprising that the hover case has a strongly different analytical form, and much slower decay versus r. Physically, this happens because the hovering rotor accumulates impulse in the field, with no mechanism to evacuate it. The static case studied here has a unique behaviour, but is certainly relevant especially for helicopters.

It is unfortunate that the range of values of A deduced from the literature is still rather wide. The primary usefulness of the finding then appears to be that it refutes the sink model (Spalart 2003 and references therein) for real turbulent flows with typical values of the distance to the outer boundary of simulations or wind-tunnel tests, normalized by rotor or nozzle diameter.

The new model can provide helpful boundary conditions for numerical simulations, both quantitatively via (2.3) (although with an uncertainty over the value of A) and in terms of setting the type of condition, between inflow and outflow, as is clear from figure 1. This figure suggests that simulations subjected to the sink flow as an inflow condition at the lower boundary will strongly conflict with it, leading to recirculation, slow convergence, and a troublesome dependence on the domain size. The model also effectively provides a non-arbitrary effective co-flow, which will help rotor and jet simulations find their statistically steady state by evacuating the starting material. It also gives an analytical initial condition, which is irrotational; this is of

https://doi.org/10.1017/jfm.2012.188 Published online by Cambridge University Press

some importance, because in unsteady simulations vorticity is conserved, and spurious initial vorticity over large slow-moving regions is quite detrimental.

The sign of the x velocity in the far-field model does not preclude having opposite flow near the rotor (Spalart 2003), where the actuator–disk sink-flow pattern becomes more dominant. This is indeed seen in simulations (Buning & Chaderjian 2011). However, at face value the $1/r$ term in (2.3) already surpasses the sink term $u_r = -Q_0/(4\pi r^2)$ at a distance of ~ 2 rotor diameters (compare Q_0 and $\mathrm{d}Q/\mathrm{d}x$), so that in practice combining the two formulas would have little value. There would be more value in adjusting the origin of the spherical coordinates used in (2.3) in the x direction, by a few rotor or nozzle diameters at the most. The large-eddy simulation in figure 2 places the virtual origin of the $1/x$ behaviour near 4.5 jet diameters. Such an adjustment is largely equivalent to adding a sink flow, since it was shown that mathematically the $1/r^2$ sink flow is the x-derivative of the new $1/r$ flow. The correct amount of adjustment can only be determined from simulations, and will depend on the type of rotor, the presence of a body, and other factors.

The likely best origin for the line of sinks in rotor cases is well below the rotor, based on the observation that the mixing begins after a few diameters of a jet. If we place that origin roughly $7R$ down, then the downwash it creates at the rotor is $\sim 1\,\%$ of the standard velocity v_h. As a result, its effect on the induced power is $1\,\%$ of the ideal value. In other words, it places an upper limit of $\sim 99\,\%$ on any rotor's figure of merit. In a similar vein, note that the direction of the vertical velocity means that formation flight is detrimental to hovering helicopters irrespective of their positions, increasing the induced power in contrast with the case of airplanes, birds, and helicopters in translation.

For jet experiments, the model indicates that the best facility will not only provide an outlet for the fluid supplied by the nozzle, but in fact an outlet for a much larger (entrained) mass flow, as well as a supply of fresh fluid, ideally distributed all around the jet. This will help control recirculations, but it will be a challenge to minimize the vorticity in this stream. Ricou & Spalding (1960) used a porous lateral wall for this purpose fifty years ago, but the practice seems to have died out. For rotor tests, a fluid supply resembling (2.2) would also reduce the errors due to using a finite facility, especially for the figure of merit, which is quite sensitive to co-flow.

Acknowledgements

Helpful comments and unpublished figures were kindly provided by Drs Shur, Strelets, and Chaderjian. Mr S. Repsher also made instructive comments, and detected an error.

REFERENCES

Buning, P. & Chaderjian, N. 2011 High resolution Navier–Stokes simulation of rotor wakes. In *67th American Helicopter Society International Annual Forum 2011*, Curran Associates, pp. 375–392.

Crow, S. C. & Champagne, F. H. 1970 Orderly structure in jet turbulence. *J. Fluid Mech.* **48** (3), 547–591.

Dziubinski, A. & Stalewski, W. 2007 Vortex ring state simulation using actuator disk. In *Proc. 21st Eur. Conf. Mod. Sim., ECMS* 2007.

Falcone, A. M. & Cataldo, J. C. 2003 Entrainment velocity in an axisymmetric turbulent jet. *J. Fluids Engng* **125**, 620–627.

Ricou, F. P. & Spalding, D. B. 1960 Measurements of entrainment by axisymmetrical turbulent jets. *J. Fluid Mech.* **11** (1), 21–32.

https://doi.org/10.1017/jfm.2012.188 Published online by Cambridge University Press

SCHLICHTING, H. 1979 *Boundary Layer Theory*. McGraw-Hill.

SHUR, M. L., SPALART, P. R. & STRELETS, M. K. 2011 LES-based evaluation of a microjet noise reduction concept in static and flight conditions. *J. Sound Vib.* **330** (17), 4083–4097.

SPALART, P. R. 2003 On the simple actuator disk. *J. Fluid Mech.* **494**, 399–405.

STEWART, R. W. 1956 Irrotational motion associated with turbulent flows. *J. Fluid Mech.* **1**, 593–606.

STRAWN, R. & AHMAD, J. 2000 Computational modelling of hovering rotors and wakes. *AIAA* paper 2000-0110.

https://doi.org/10.1017/jfm.2012.188 Published online by Cambridge University Press